Int. J. Environ. Sci. Technol. (2016) 13:2269–2282
DOI 10.1007/s13762-016-1059-3

ORIGINAL PAPER

Ionic solid-impregnated sulphate-crosslinked chitosan for effective adsorption of hexavalent chromium from effluents

S. Kahu[1] · A. Shekhawat[1] · D. Saravanan[2] · R. Jugade[1]

Received: 7 April 2015 / Revised: 13 February 2016 / Accepted: 27 June 2016 / Published online: 12 July 2016

Abstract Microwave-assisted tetrabutyl ammonium-impregnated sulphate-crosslinked chitosan was synthesized for enhanced adsorption of hexavalent chromium. The adsorbent obtained was extensively characterized using Fourier transform infrared, X-ray diffraction, scanning electron microscopy and energy-dispersive X-ray studies. Various isotherm models such as Langmuir, Freundlich and Dubinin–Radushkevich were studied to comprehend the adsorption mechanism of hexavalent chromium by the adsorbent. Maximum adsorption capacity of 225.9 mg g^{-1} was observed at pH 3.0 in accordance with Langmuir isotherm model. The sorption kinetics and thermodynamic studies revealed that adsorption of hexavalent chromium followed pseudo-second-order kinetics with exothermic and spontaneous behaviour. A column packed with 1 g of adsorbent was found to give complete adsorption of Cr(VI) up to 900 mL of 200 mg L^{-1} solution which discerns the applicability of the adsorbent material for higher sample volumes in column studies. The effective adsorption results were obtained due to both ion exchange and ion pair interaction of adsorbent with hexavalent chromium. Greener aspect of overall adsorption was regeneration of the adsorbent which was carried out using sodium hydroxide solution. In the present study, the regenerated adsorbent was effectively reused up to ten adsorption–desorption cycles with no loss in adsorption efficiency.

Keywords Biosorption · Carcinogen · Detoxification · Tetrabutyl ammonium bromide

✉ R. Jugade
ravinj2001@yahoo.co.in

[1] Department of Chemistry, R.T.M. Nagpur University, Nagpur 440033, India

[2] Department of Chemistry, National College, Tiruchirappalli 620001, India

Introduction

At present, heavy metal pollution in environment is of great concern towards the health of human beings. Chromium is not an omission. Generally chromium exists in trivalent Cr(III) and hexavalent Cr(VI) states. Cr(III) is an essential nutrient for human being, whereas Cr(VI) is a potent carcinogen (Katz and Salem 2006). Effluents from electroplating, tannery and dyeing industries contain Cr(VI) (Lewinsky 2007). Permissible limit of Cr(VI) in drinking water is 0.05 mg L^{-1}. Therefore, there is a need to develop more effective methodology for detoxification of Cr(VI).

Chitosan is a natural polyaminosaccharide. Source material for chitosan is chitin which is the second most abundant biopolymer after cellulose. Chitin is an important constituent of some fungi and exoskeletons of crustaceans, molluscs and insects. Chitosan has monomer units of glucosamine and *N*-acetyl glucosamine linked by β(1–4) glycosidic bonds. Its glucosamine content refers to the degree of deacetylation, and it is generally more than 60 %. Properties of chitosan such as biocompatibility, biodegradability and good adsorption tendency make it good material for wastewater treatment (Bhatnagar and Sillanpaa 2009).

Chitosan has gained pronounced attention in the field of biosorption that can be attributed to its chemical stability, high reactivity, excellent chelation behaviour and high selectivity towards pollutants (Elwakeel 2014; Geetha Devi et al. 2012). A modification of chitosan mainly involves the free-amine group on deacetylated units and hydroxyl

groups on C_3 and C_6 carbons of monomers units (Kyzas and Bikiaris 2015). These groups of chitosan can be grafted or crosslinked with organic and inorganic moieties for removal of Cr(VI) (Debnath et al. 2014; Tirgar et al. 2006). A sulphate-crosslinked chitosan for detoxification of chromium has been prepared by Kahu et al. (2014). Anchoring of trialkyl amines on adsorbent has been reported in literature for the solid phase extraction of Cr(VI) (Kumar et al. 2015). Crosslinking provides mechanical strength and stability to the material while impregnation provides enhanced interaction with Cr(VI). Combination of these two modifications has a synergistic effect leading to improvement in adsorbent properties (Shekhawat et al. 2015).

Microwave-enhanced chemical reaction rates are faster than those of conventional heating methods and provide more effective means of energy transfer (Hayes 2004). Solvent-free preparation of surfactant–anchored cellulose towards chromium adsorption by using microwave irradiation has been reported by Kalidhasan et al. (2012). Microwave-assisted grafting of *n*-butyl acrylate on chitosan for Cr(VI) adsorption is an example of grafting on chitosan (Kumar et al. 2014a). In present study, tetrabutyl ammonium bromide-impregnated sulphate-crosslinked chitosan (TBA-SCC) has been synthesised by crosslinking polymer chains of chitosan with sulphate ions followed by impregnation of tetrabutyl ammonium bromide using microwave irradiation.

Materials and methods

This research project has been carried out in Analytical chemistry laboratory, Department of chemistry, R.T.M. Nagpur University, Nagpur from October 2014 to January 2015.

Tetrabutyl ammonium bromide (TBAB), Diphenyl carbazide, sulphuric acid, sodium hydroxide and potassium dichromate were procured from Merck, India. Aqueous solutions were prepared using double-distilled water. Uniloid Bio-Chemicals India Limited, Hyderabad, supplied chitosan having 85 % of degree of deacetylation. All the reagents were of analytical grade and used without further purification.

Preparation of TBAB-impregnated sulphate-crosslinked chitosan (TBA-SCC)

Sulphate-crosslinked chitosan (SCC) was prepared as reported in the literature (Kahu et al. 2014); 5 g of chitosan powder was treated with 100 mL of 4 % *v*/*v* sulphuric acid in a round bottom flask and stirred at room temperature for 1 h. SCC obtained after filtration was washed several times with double-distilled water and dried at 333 K in hot air oven. An ordinary household microwave oven (LG India) was used for impregnation of TBAB on SCC. For this, 2.0 g SCC was taken in conical flask and to it 5 mL of 0.5 M TBAB solution in dichloromethane was added. The reaction mixture was stirred, and then it was subjected to microwave irradiation for 2 min with an intermittent time interval of 30 s. The resulting residue (TBA-SCC) was washed with double-distilled water and dried at 333 K in hot air oven and was used for further adsorption studies.

Physico-chemical characterization

Structure of TBA-SCC could be explained on the basis of Fourier transform infrared (FTIR) spectra recorded using Bruker Alpha spectrometer in the range 500–4000 cm^{-1}. The X-ray diffraction (XRD) pattern was recorded by X-ray diffractometer system Righaku–Miniflex 300. Surface morphology of adsorbent prior and consequent to adsorption of Cr(VI) was studied using scanning electron microscope (SEM) model TESCAN VEGA 3 SBH. Energy-dispersive spectral (EDX) analysis was performed for elemental quantitation using X-ray analyzer Oxford INCA Energy 250 EDS System during SEM observations.

Standard diphenylcarbazide method (Mendham et al. 2002) at 540 nm was utilized for spectrophometric determination of Cr(VI) concentration in solution phase after adsorption using Spectronic 20D+ spectrophotometer. pH adjustments were made with dilute sulphuric acid and sodium hydroxide solutions using an Equiptronics model EQ-615 pH meter.

Adsorption procedure

Adsorption studies were performed by using varying concentrations of Cr(VI) from 50 to 800 mg L^{-1} maintaining all the optimized parameters such as pH, adsorbent dose and contact time and temperature constant.

The amount of Cr(VI) adsorbed (mg g^{-1}) on TBA-SCC at equilibrium (q_e) can be given by

$$q_e = \frac{C_0 - C_e}{W} \times V \quad (1)$$

where C_0 and C_e specify the initial and equilibrium liquid-phase concentrations in mg L^{-1} of Cr(VI), V is the volume of Cr(VI) solution in litres, and W is the weight of TBA-SCC in gram used for adsorption process. All the batch adsorption experiments were performed with three replicates.

Desorption and reusability experiments

The adsorbent along with adsorbed Cr(VI) was treated with 2 % NaOH solution to break down the impregnation as

well as crosslinking in TBA-SCC and regenerate chitosan. This was further converted into TBA-SCC as explained above.

Results and discussion

FTIR spectral characterization

The FTIR spectral analysis (Fig. 1) showed distinct characteristic broad peaks corresponding to the various functional groups in chitosan and modified chitosan derivatives: O–H and N–H stretching vibrations in the region 3808 and 3276 cm^{-1}, the N–H bending vibration around 1556 cm^{-1}, C–N bending vibration at 1379 cm^{-1} and the C–H and C–O stretching bands around 2868 and 1012 cm^{-1}. In SCC, sulphate group peaks appeared at around 607 cm^{-1} in accordance with reported literature (Mayyas 2012). After impregnation with tetrabutyl ammonium bromide, two additional peaks were appeared at 2999 and 2805 cm^{-1} corresponding to the $–CH_2$ groups of aliphatic chains confirming the impregnation. The quaternary ammonium ion of TBAB and sulphate ion of TBA-SCC are responsible for Cr(VI) adsorption. After adsorption of Cr(VI), a new peak was observed at 942 cm^{-1} which matches with reported value (Kumar et al. 2014b).

XRD studies

The diffraction patterns (Fig. 2) of SCC, TBA-SCC and with adsorbed Cr(VI) were recorded for characterization of adsorbent and to understand the feasibility of adsorption of Cr(VI) on adsorbent. XRD spectra of SCC showed characteristic peaks at $2\theta = 11.4°$, 18.2° and 23.7°. In the case of TBA-SCC, these peaks were found to get shifted to $2\theta = 12.12°$, 19.0° and 23.64°, respectively. These changes in the 2θ angle are mainly due to the decrease in crystallinity of the adsorbent which accounts for interaction of tetrabutyl ammonium bromide with SCC. After adsorption of Cr(VI) on TBA-SCC, an additional peak was observed at $2\theta = 26.8°$ which matches with the reported value for Cr(VI) (Kahu et al. 2014).

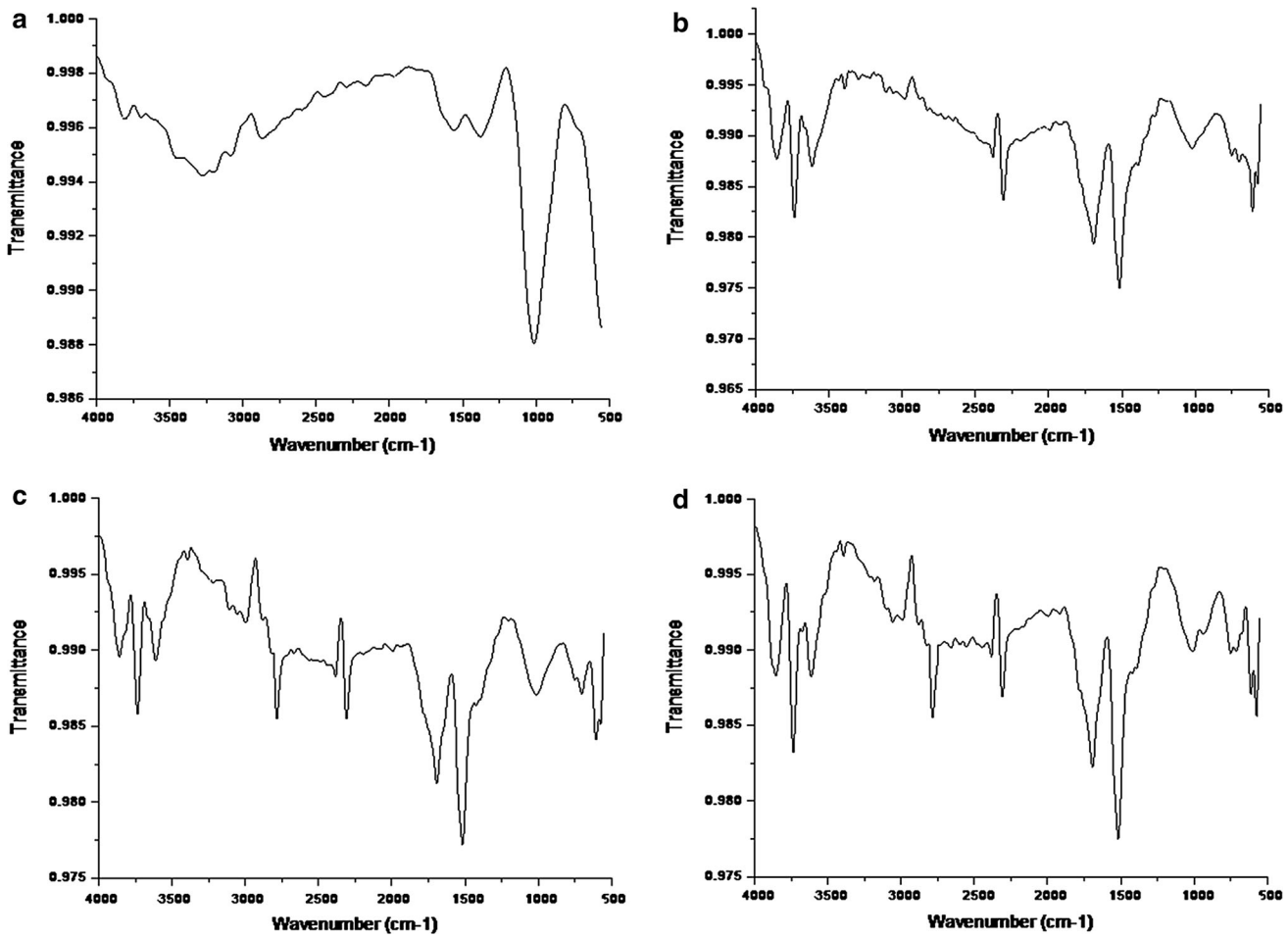

Fig. 1 FTIR spectrum of **a** chitosan, **b** SCC, **c** TBA-SCC, **d** TBA-SCC with adsorbed chromium

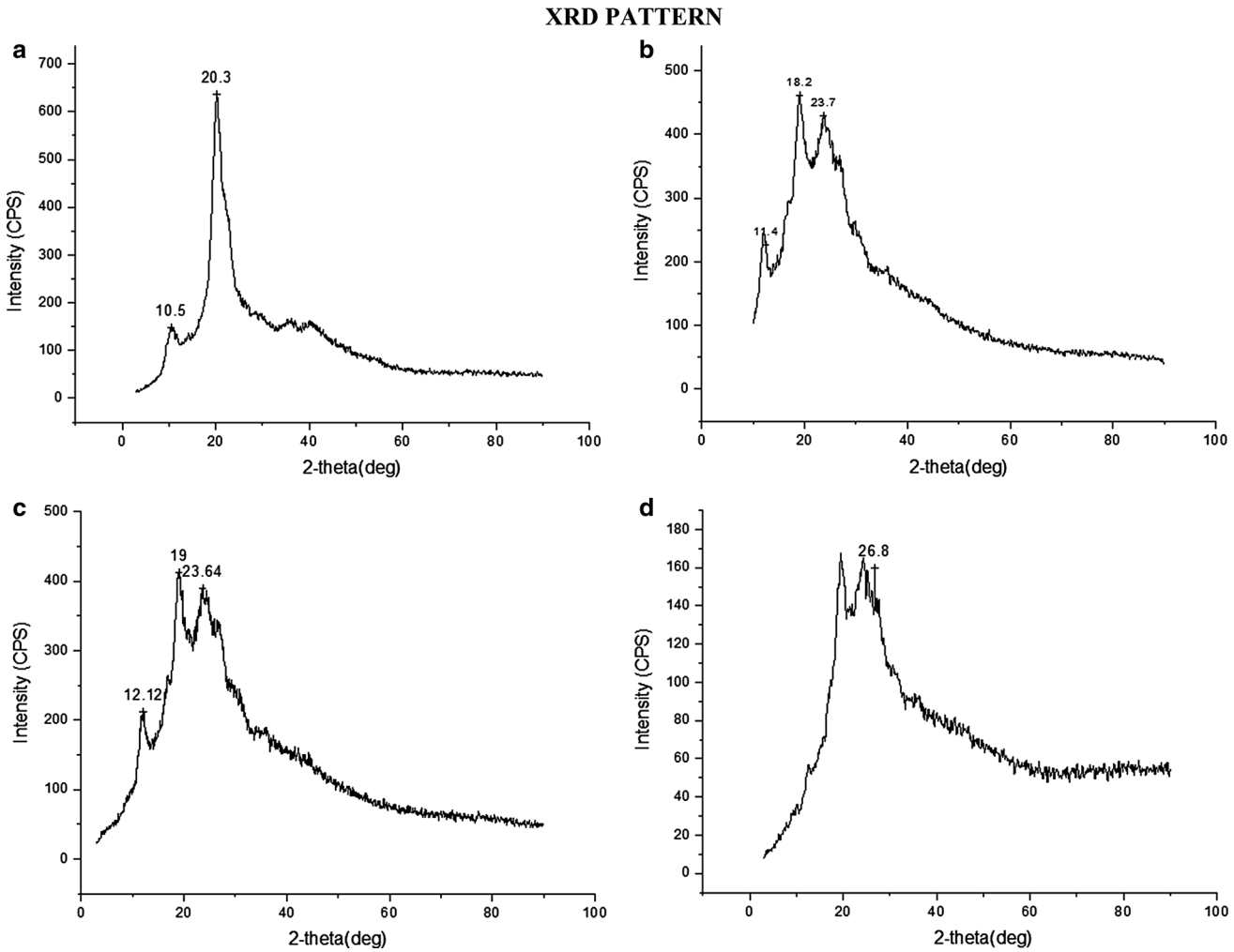

Fig. 2 XRD pattern **a** chitosan, **b** SCC, **c** TBA-SCC, **d** After adsorption of Cr(VI)

Morphology of adsorbent using SEM and EDX spectral analysis

SEM micrographs (Fig. 3a) define the morphology of the adsorbent material. SCC exhibits regular and dense surfaces and became uniformly porous after impregnation with tetrabutyl ammonium bromide. SEM micrographs of the TBA-SCC with adsorbed Cr(VI) show glossy and bright spots indicating effective interaction of Cr(VI) with the adsorbent.

EDX spectra (Fig. 3b) of SCC, TBA-SCC and with adsorbed Cr(VI) confirmed the Cr(VI) adsorption. In Cr(VI)-adsorbed TBA-SCC characteristic peaks, K_α and K_β of Cr(VI) along with the peaks of other elemental constituents such as sulphur, carbon, nitrogen, oxygen have been observed.

Effect of contact time

Effect of contact time on the adsorption of Cr(VI) concentration of 50 mg L^{-1} was studied by varying the contact time in the range 5–90 min at 298 K. The rate of removal of Cr(VI) was found to be higher at the beginning while the equilibrium is reached in about 60 min. Equilibrium was accomplished with adsorption of 99.6 ± 0.1 % Cr(VI) in 60 min (Fig. 4a) which was fixed as contact time for further studies.

% Removal of Cr(VI) can be calculated as

$$\%\,\text{Removal} = \frac{C_0 - C_e}{C_0} \times 100 \quad (2)$$

where C_0 and C_e refer to the initial and equilibrium liquid-phase concentrations of Cr(VI) in mg L^{-1}.

Effect of adsorbent amount

The effect of TBA-SCC dose on adsorption efficiency was studied by varying its amounts from 50 to 400 mg (Fig. 4b). Initially, due to greater interaction of dichromate ion and the adsorbent, % removal of Cr(VI) increases rapidly. Beyond 200 mg of TBA-SCC dose, unavailability

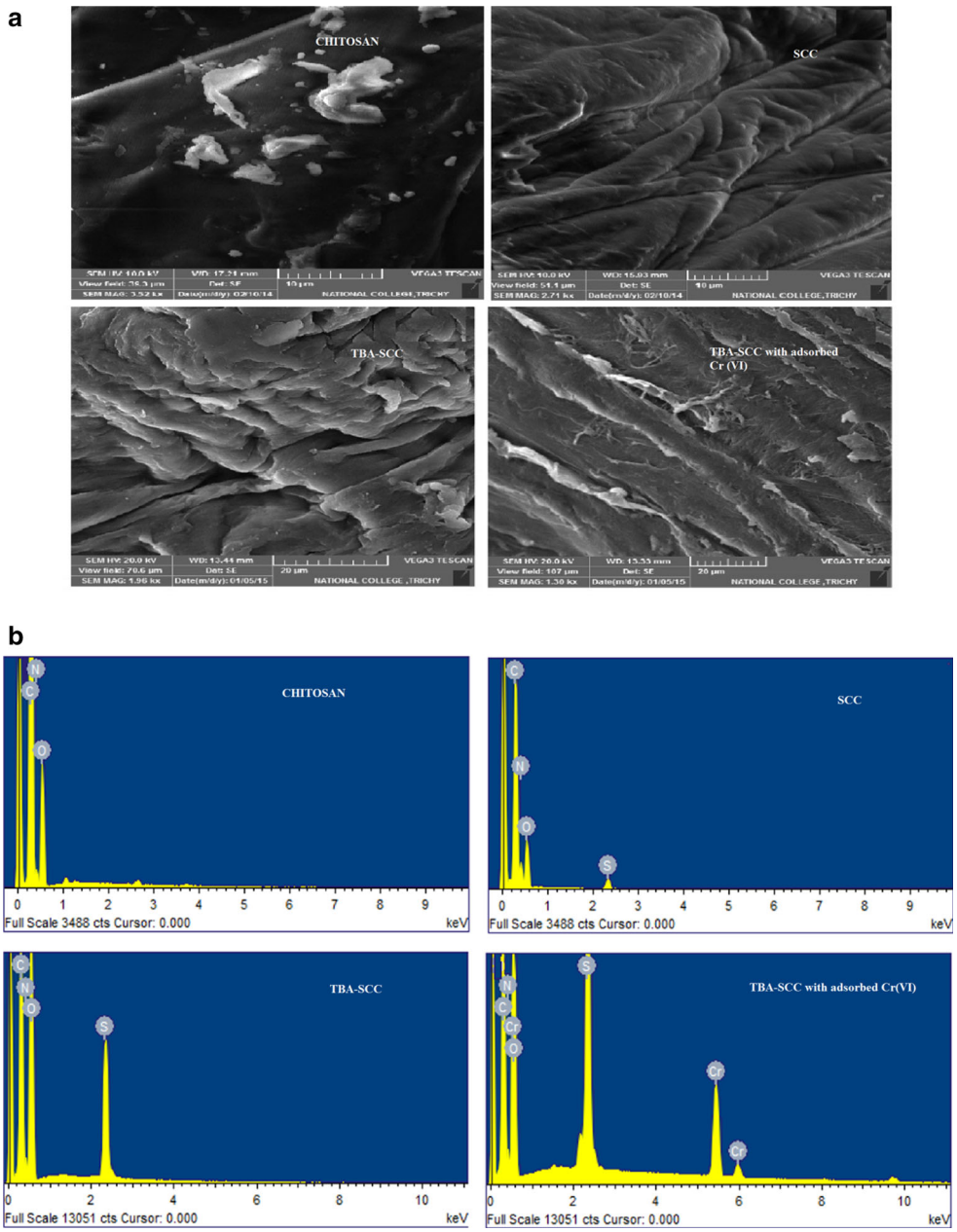

Fig. 3 **a** SEM micrographs and **b** EDX spectra of chitosan and modified chitosan with Cr(VI)

of adsorbate resulted in no observable rise in removal of Cr(VI). Hence, dose of 200 mg was fixed for further adsorption studies.

Effect of initial Cr(VI) concentration

At different initial Cr(VI) concentrations (20–300 mg L^{-1}) with fixed contact time (60 min) and TBA-SCC dosage (200 mg), adsorption experiments were performed. Up to 50 mg L^{-1} of Cr(VI), the % removal was found almost steady and then it started decreasing due to the saturation of adsorbent (Fig. 4c). Therefore, 50 mg L^{-1} Cr(VI) solution was used for further adsorption studies.

pH point of zero charge

The pH at which the surface charge of the adsorbent became zero is known as pH point of zero charge (pH_{PZC}). pH_{PZC} of the adsorbent was determined by batch equilibration technique (Shekhawat et al. 2016). For this, 50 mL of 0.1 M NaCl solution was taken in a series of conical flasks and its initial pH was adjusted from 2.0 to 9.0 using dilute H_2SO_4 and NaOH solutions. These solutions were equilibrated with 100 mg of TBA-SCC adsorbent for a period of 24 h, and the final pH values of supernatant solutions were measured. The pH_{PZC} of the TBA-SCC was evaluated from the plot of ΔpH [$pH_{initial}$–pH_{final}] versus

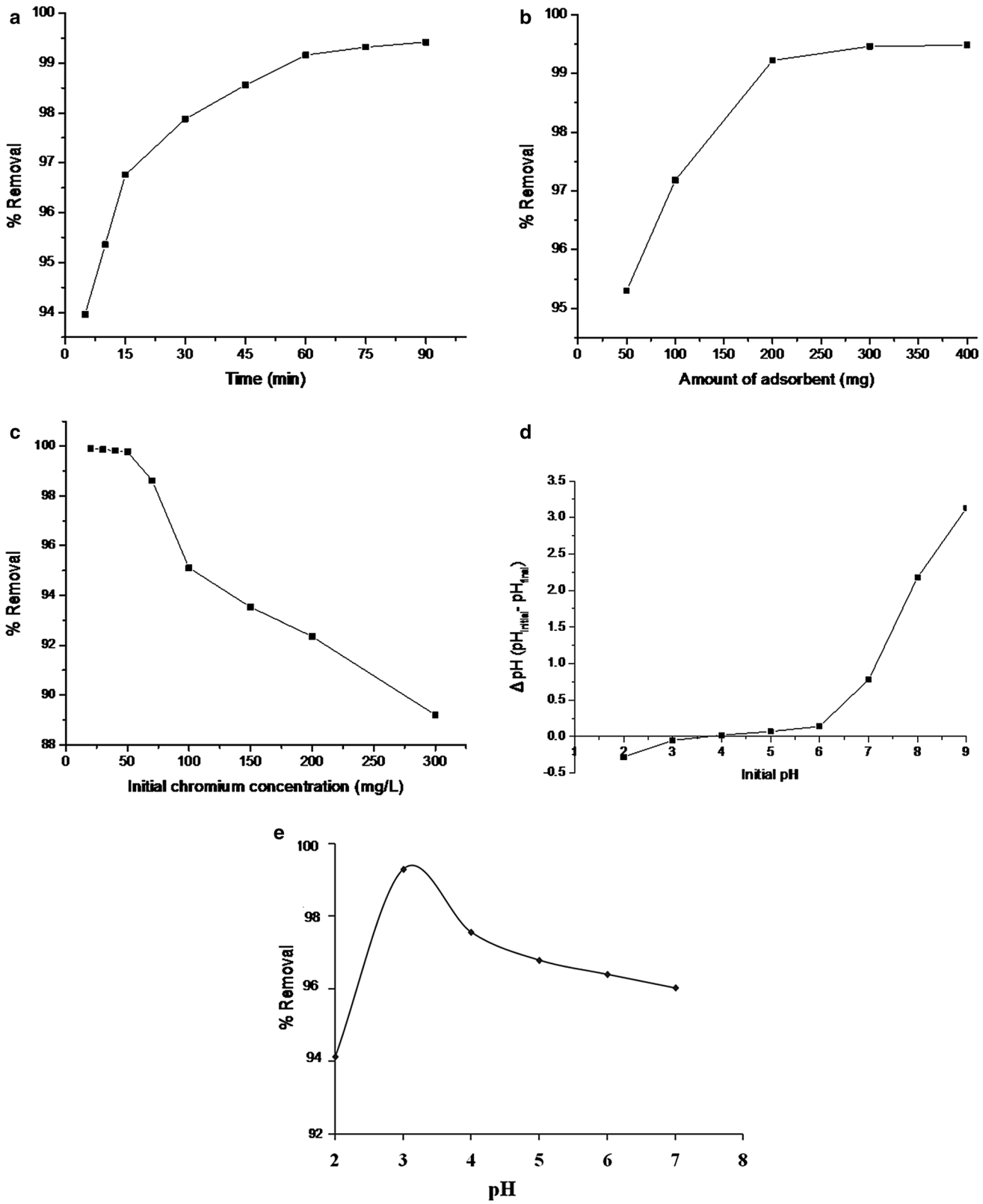

Fig. 4 Effect of **a** contact time, **b** adsorbent dose, **c** initial concentration, **d** pH point of zero charge and **e** pH on adsorption efficiency

$pH_{initial}$. For TBA-SCC, the pH_{PZC} was found to be 3.7 (Fig. 4d). It means that the adsorbent surface is positively charged below pH 3.7 and negatively charged above this pH.

Effect of pH

Optimizing the pH is a significant parameter while assessing the adsorption capacity of an adsorbent. In aqueous medium, Cr(VI) mainly exists in different forms such as hydrogen chromate ($HCrO_4^-$), dichromate ($Cr_2O_7^{2-}$) and chromate (CrO_4^{2-}). The equilibrium exists between these anions depending on pH (Zhu et al. 2009) as follows:

$$H_2CrO_4 \rightleftharpoons H^+ + HCrO_4^-$$
$$HCrO_4^- \rightleftharpoons H^+ + CrO_4^{2-}$$
$$2HCrO_4^- \rightleftharpoons Cr_2O_7^{2-} + H_2O$$

Also, the speciation of adsorbate and surface charge of the adsorbent can be related to pH. The pH of the solution was varied from 2.0 to 7.0 at constant initial concentration of 50 mg L^{-1} of Cr(VI), contact time of 60 min and 298 K temperature. It was found that the % removal was maximum at pH 3.0 ± 0.1 (Fig. 4e) which favours the formation of dichromate anion and also protonation of the surface nitrogen-containing group. Dichromate anion shows ion pair interaction with $N^+(C_4H_9)_4$ of TBA-SCC and also gets exchanged with crosslinked sulphate ions of the adsorbent. At this pH condition, the surface of adsorbent is positively charged (below pH_{PZC}) that favours electrostatic interaction with dichromate ion.

Adsorption isotherms

Various adsorption isotherm models such as Langmuir, Freundlich and Dubinin–Radushkevich (D–R) were studied quantitatively. The adsorption studies were carried out by equilibrating 50 mL of varying initial Cr(VI) concentrations (100–800 mg L^{-1}) at pH 3.0 with 200 mg of TBA-SCC at 298 K for 60 min.

The purpose of Langmuir isotherm model study is to understand the monolayer adsorption on homogeneous surface and to calculate the maximum adsorption capacity of adsorbent (Langmuir 1918). It relates the maximum adsorption capacity (q_0) and the Langmuir constant related to affinity of binding sites (b) in linearized Langmuir equation:

$$\frac{C_e}{q_e} = \frac{1}{q_0 b} + \frac{C_e}{q_0} \quad (3)$$

The maximum adsorption capacity q_0 and the constant b were obtained from the slope and intercept of the plot of C_e/q_e against C_e (Fig. 5a). A high adsorption capacity of 225.9 mg g^{-1} accounts for excellent adsorption behaviour of TBA-SCC adsorbent for Cr(VI). A separation factor R_L that relates to the favourable nature of adsorption is given by the following equation:

$$R_L = \frac{1}{1 + bC_o} \quad (4)$$

R_L value less than unity (Table 1) indicating effective interaction (Crini et al. 2007) between the TBA-SCC and Cr(VI) at the optimized experimental conditions.

Inequivalent adsorbent sites lead to surface heterogeneity during adsorption, which has been explained by Freundlich isotherm model (Freundlich 1906). k_F refers to adsorption capacity, and n indicates the adsorption intensity with the linearized expression given as

$$\log q_e = \log k_F + \frac{1}{n} \log C_e \quad (5)$$

The logarithmic plot of q_e against C_e gives the constants k_F and n (Fig. 5b). The smaller value of $1/n$ 0.614 ($0.1 < 1/n < 1.0$) (Table 1) signifies an active interaction between TBA-SCC and Cr(VI) (Kumar and Rajesh 2013).

Dubinin–Radushkevich isotherm is commonly used to predict the type of adsorption mechanism and the interaction between the adsorbate and adsorbent (Dubinin and Radushkevich 1947). The D–R isotherm parameters β a constant related to adsorption energy and ε, Polyani potential is expressed as

$$\ln q_e = \ln q_m - \beta\varepsilon^2 \quad (6)$$

where q_m (mg g^{-1}) is the adsorption capacity. The intercept and slope in plot of ln q_e verses ε^2 give the values of q_m and β, respectively (Fig. 5c). The value of ε was calculated using following equation

$$\varepsilon = RT \ln\left(1 + \frac{1}{C_e}\right) \quad (7)$$

where R (8.314 J mol^{-1} K^{-1}) is a gas constant and T (K) is absolute temperature. The mean free adsorption energy was calculated by the following equation:

$$E = -\left(\frac{1}{(2\beta)^{0.5}}\right) \quad (8)$$

In the present work, the value of E was found to be −6.47 kJ mol^{-1}. This value reflects both chemisorption and physisorption. Value of β, E and q_m was depicted in Table 1.

The values of regression coefficient (Table 1) and the plot of experimental q_e along with q_e values of all the isotherms against C_e (Fig. 5d) implie that the Freundlich isotherm model has good agreement with experimental q_e

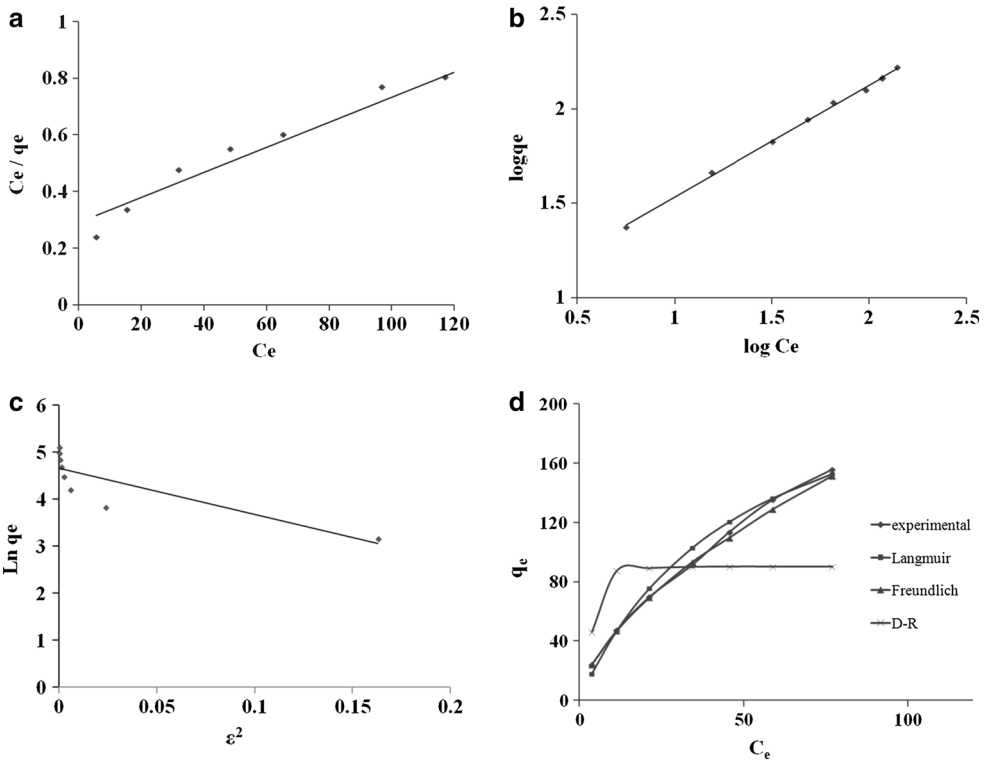

Fig. 5 Adsorption isothems: **a** Langmuir, **b** Freundlich, **c** D–R, **d** comparison of experimental q_e with other isotherms

Table 1 Isotherm parameters acquired from various models

Sl. no.	Isotherms	Parameters	Values
1.	Langmuir	q_0 (mg g^{-1})	225.9
		b (L mg^{-1})	0.015
		R_L	0.567
		r^2	0.950
2.	Freundlich	K_F ($mg^{1-1/n}$ g^{-1} L^{-1})	10.62
		n	1.679
		r^2	0.997
3.	Dubinin Radushkevich	q_m (mg g^{-1})	109.69
		β (mol^2 kJ^{-2})	4.82E−6
		E (kJ mol^{-1})	−6.47
		r^2	0.704

with highest value for regression coefficient. Thus, Freundlich isotherm was the best fit model for adsorption of Cr(VI) by TBA-SCC which assumes heterogeneous multilayer adsorption.

Kinetics of adsorption

The amount of metal ion adsorbed by the adsorbent depends on the contact time, and thus, kinetics of adsorption of Cr(VI) on to the TBA-SCC was explained through pseudo-first-order and pseudo-second-order kinetic models. The studies were carried out using 50 mL, 50 mg L^{-1} Cr(VI) solution at pH 3.0. It was equilibrated with 200 mg of TBA-SCC at 298 K for different time intervals (5–90 min).

The pseudo-first-order kinetics (Lagergren 1898) is given by the equation

$$\log(q_e - q_t) = \log q_e - \frac{k_1 t}{2.303} \quad (9)$$

where q_e and q_t refer to the amounts of Cr(VI) adsorbed at equilibrium and at time t with the first-order rate constant k_1. The plot of log $(q_e - q_t)$ against t gives pseudo-first-order rate constant with regression coefficient 0.766 (Fig. 6a).

The pseudo-second-order equation (Ho 2006) is given as

$$\frac{t}{q_t} = \frac{1}{k_2 q_e^2} + \frac{t}{q_e} \quad (10)$$

where k_2 is the pseudo-second-order rate constant in g mg^{-1} min^{-1}. The plot of log t/q_t against t (Fig. 6b) gives pseudo-second-order rate constant. Regression coefficient of 0.999 for pseudo-second-order rate kinetics offers a best fit model to describe the adsorption of Cr(VI) on to TBA-SCC.

During adsorption whether intraparticle diffusion is the rate-determining step can be confirmed by Weber–Morris model (Weber and Morris 1963). According to this model, q_t and $t^{1/2}$ of adsorption process are related as:

$$q_t = k_{int} \cdot t^{1/2} + C \quad (11)$$

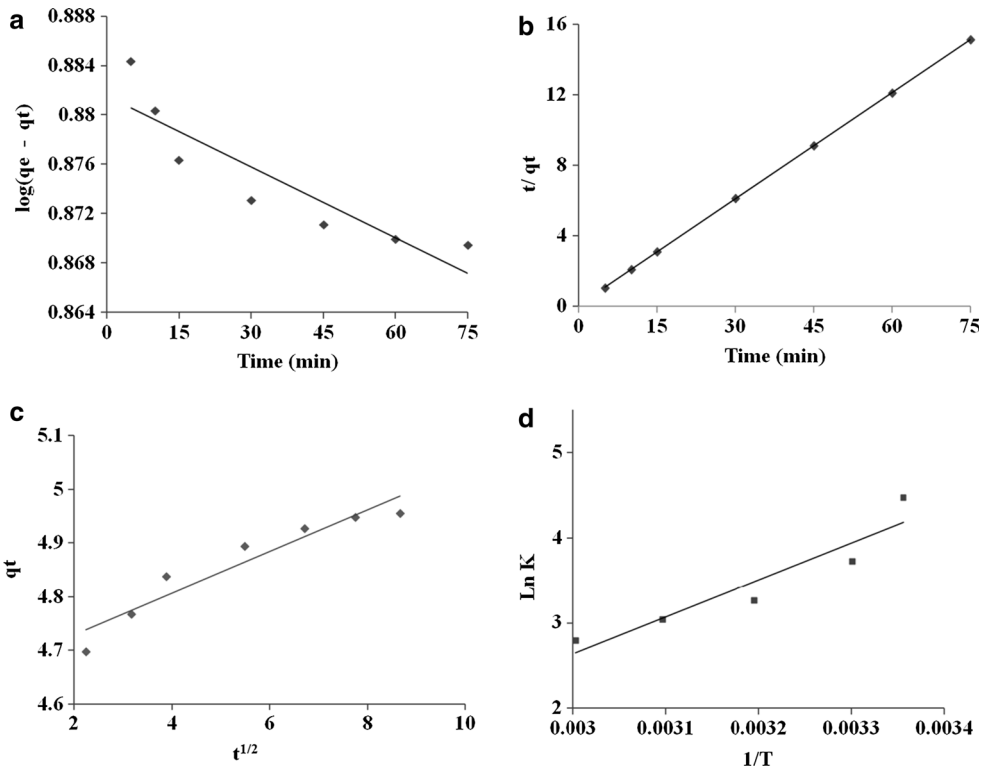

Fig. 6 Kinetic and thermodynamic studies: **a** pseudo-first-order kinetics, **b** pseudo-second-order kinetics, **c** intraparticle diffusion, **d** van't Hoff plot

If the plot of q_t verses $t^{1/2}$ (Fig. 6c) passes through origin and is linear, then intraparticle diffusion is the only rate-limiting step. The slope gives the intraparticle rate constant k_{int} (Table 2), and nonzero intercept showed that diffusion is not the only rate-limiting step. Rate of adsorption of Cr(VI) may be influenced by external mass transfer of Cr(VI) from solution phase to solid phase, pore diffusion and at interior sites of the adsorbent. Thus, the adsorption of Cr(VI) by TBA-SCC was controlled by boundary layer as well as diffusion process (Bulut et al. 2008).

Thermodynamics of adsorption

Effect of temperature on adsorption of Cr(VI) by TBA-SCC was studied in order to obtain relevant thermodynamic parameters at 298, 303, 308, 318 and 328 K. These parameters describe the spontaneous nature of adsorption. The free energy change of adsorption ($\Delta G°$) is given by

$$\Delta G^0 = -RT \ln K \tag{12}$$

van't Hoff equation (Donia et al. 2006) which relates entropy ($\Delta S°$) and enthalpy ($\Delta H°$) changes is given by

$$\ln K = \frac{\Delta S^0}{R} - \frac{\Delta H^0}{RT} \tag{13}$$

where R is the gas constant (8.314 J mol^{-1} K^{-1}). The value of equilibrium constant K has been evaluated from the ratio of concentration of Cr(VI) adsorbed to that in the solution phase. The values of ΔH and ΔS (Table 2) were obtained from slope and intercept of the plot of ln K against $1/T$ (Fig. 6d), respectively. The negative free energy change indicates the spontaneous nature, negative enthalpy change indicates the exothermic nature of adsorption process, while negative entropy change indicates the decrease in randomness of Cr(VI) as it passes from solution to adsorbed state.

Column studies

Column adsorption studies were performed by using glass column of 30.0 cm length, and 1.0 cm inner diameter was used to understand the applicability of adsorbent for larger sample volumes. Column was packed with 1.0 g of adsorbent to the height of 6.0 cm. 1500 mL of 200 mg L^{-1} Cr(VI) solution was passed through the column at the flow rate of 5 mL min^{-1}. Concentration of Cr(VI) in solution phase was analysed spectrophotometrically to quantify the column efficiency. Adsorption of Cr(VI) was found to be almost 100 % up to 900 mL of 200 mg L^{-1} Cr(VI) (Fig. 7) solution. The identical results were obtained in three replicates. These results clearly indicate that larger sample volumes containing Cr(VI) can be effectively treated using column method compared to batch extraction.

Table 2 Kinetics and thermodynamic parameters

Kinetics parameters					
Pseudo-first-order kinetics		Pseudo-second-order kinetics		Intraparticle diffusion	
k_1 (min^{-1})	Regression coefficient	k_2 (g mg^{-1} min^{-1})	Regression coefficient	k_{int} (mg g^{-1} $min^{-1/2}$)	Regression coefficient
0.0002	0.813	0.095	0.999	0.038	0.911

Thermodynamic parameters			
Temperature	ΔG (kJ mol^{-1})	ΔH (kJ mol^{-1})	ΔS (kJ mol^{-1} K^{-1})
298 K	−11.10	−36.041	−0.0862
303 K	−9.39		
308 K	−8.51		
318 K	−8.16		
328 K	−7.37		

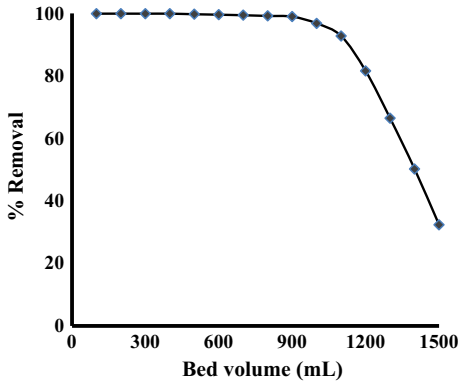

Fig. 7 Effect of bed volume on column efficiency

Effect of assorted ions

The real effluent wastewater contains varied anions and cations which may compete for the accessible active sites on the TBA-SCC surface. Hence, it is important to study the effect of individual ion on selectivity towards Cr(VI). Various anions such as SO_4^{2-}, Cl^-, NO_3^-, PO_4^{3-} and cations such as Cu^{2+}, Ni^{2+}, Co^{2+}, Zn^{2+}, Fe^{2+} and Fe^{3+} present in a real wastewater were tested for their effect on adsorption of Cr(VI) by TBA-SCC. For this, adsorption studies were carried out using 50 mL of 1 mM Cr(VI) solution in the presence of equimolar interfering ions under optimized conditions. From Fig. 8a, b, it is clear that the Cl^- and Fe (total) interfere to the greatest extent among these ions.

Regeneration and reusability of adsorbent

The regeneration of adsorbent is important from a greener point. Reagents such as sodium hydroxide, sodium carbonate and sulphuric acid were examined for desorption studies. In the present study, the regenerated TBA-SCC is effectively used for ten adsorption–desorption cycles with no change in adsorption capacity compared to freshly prepared TBA-SCC (Fig. 8c). The best results were obtained with 2 % (*w*/*v*) NaOH solution (Fig. 8d). 2 g of TBA-SCC with adsorbed Cr(VI) was taken in round bottom flask, to it 50 mL of 2 % NaOH solution was added and boiled for 30 min. The reaction mixture was cooled, filtered and then washed with distilled water to regenerate chitosan (checked by IR characterization of the residue). It clearly indicates that the crosslinking as well as impregnation breaks down at high pH of NaOH solution. It could be further modified to TBA-SCC and the regenerated compound was found to have the same adsorption efficiency (Fig. 8e).

Applicability to synthetic effluent

In order to confirm the applicability of TBA-SCC for removal of Cr(VI), three different synthetic effluents were prepared having similar composition to that of real effluents and adsorption efficiency was determined (Rajesh et al. 2011). The cations such as Ni^{2+}, Cu^{2+}, Co^{2+}, Zn^{2+}, Fe^{2+}, Fe^{3+} and anions as Cl^-, SO_4^{2-}, NO_3^-, PO_4^{3-} present in effluents affect the adsorption efficiency. These ions may interfere and alters the adsorption capacity. The results have been depicted in Table 3. More than 94 % removal of Cr(VI) was observed in single batch extraction which may further be improved using multiple extractions. The used adsorbent was analysed by EDX. The spectrum (Fig. 9) clearly shows the presence of chloride ions indicating their involvement in the adsorption process.

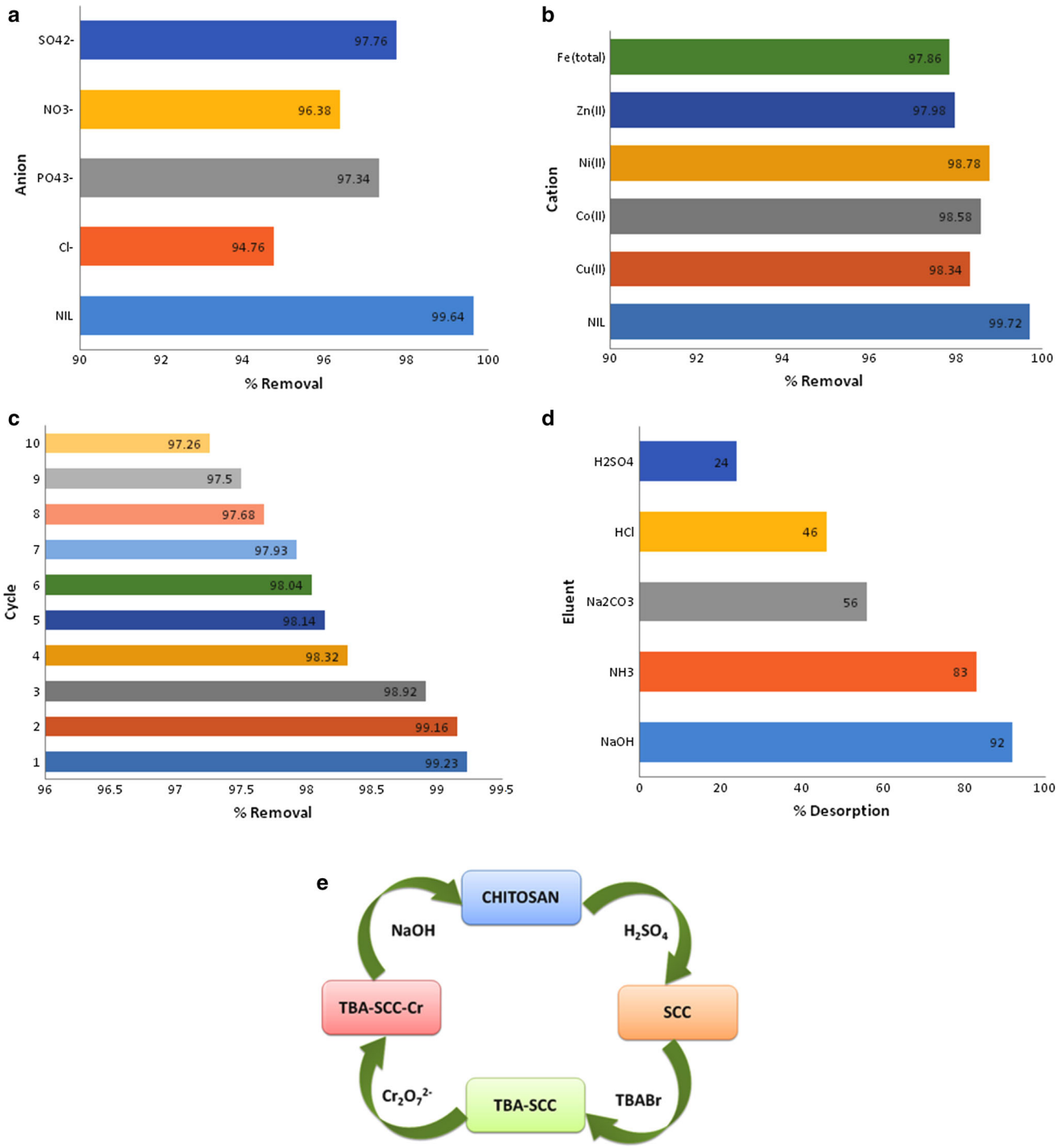

Fig. 8 Effect of **a** anion, **b** cation on % removal of Cr(VI), **c** regeneration cycles, **d** desorption studies, **e** mechanism of regeneration

Mechanism of adsorption of Cr(VI) by TBA-SCC

In TBA-SCC, sulphate ions and $N^{+}(C_4H_9)_4$ are juxtaposed in such a manner to facilitate the effective adsorption of dichromate ions. In the host–guest complexation phenomena, the resulting binding energies were due to the electrostatic and van der Waals interactions (Houk et al. 2003). In present work, Cr(VI) adsorption shows concurrent behaviour involves ion pair interactions with $N^{+}(C_4H_9)_4$ and ion exchange

Table 3 Application of TBA-SCC to synthetic effluents

Synthetic effluent	Concentration of ions (mg L^{-1})	% Removal of chromium
1	Cl^-(750), SO_4^{2-}(859), NO_3^-(100), Mn^{2+}(750), Fe^{2+}(500), total Cr(200)	96.2 ± 0.2
2	Cl^-(605), SO_4^{2-}(1375), NO_3^-(500), Zn^{2+}(500), Fe^{2+}(350), Ni^{2+}(500), total Cr(200)	97.5 ± 0.2
3	Cl^-(953), SO_4^{2-}(1041), NO_3^-(700), Fe^{2+}(100), Fe^{3+}(500), Ni^{2+}(500), total Cr(200)	94.1 ± 0.3

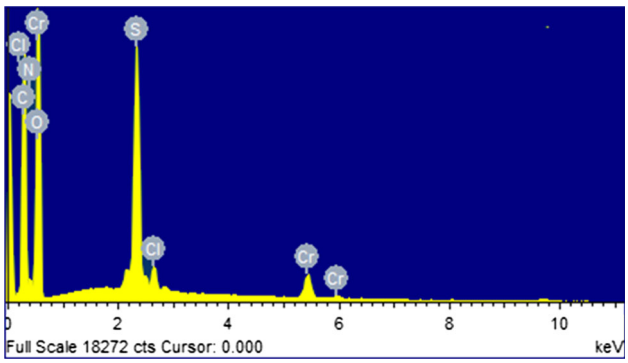

Fig. 9 EDX spectrum of adsorbent after adsorption of Cr(VI) in synthetic effluent

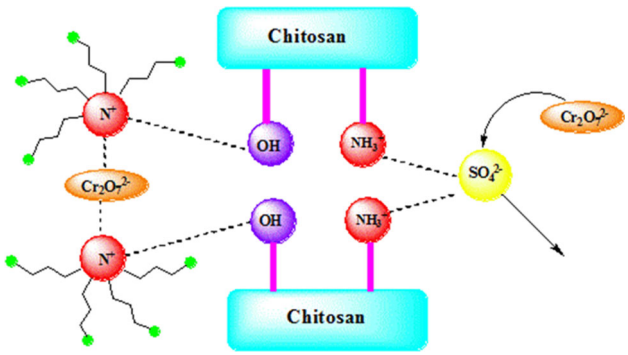

Fig. 10 Mechanism of adsorption

phenomena with sulphate ions of TBA-SCC (Fig. 10). Ion exchange phenomena were predicted by the sulphate ions detection in the remaining aqueous medium after the adsorption of Cr(VI).

Comparison with other related adsorbents

The adsorption capacity is a yardstick to assess an adsorbent. The adsorption capacity of TBA-SCC is higher than some of the other reported biopolymer adsorbents (Table 4).

Conclusion

Generally impregnation of an adsorbent will take 4 h with simple conventional method (Kumar et al. 2014a, b). Present work has demonstrated that the impregnation could be performed in 2 min by using domestic microwave and the resulting adsorbent has high adsorption efficiency. The interaction between the SCC and tetrabutyl ammonium bromide enhances the potential application of adsorbent for the effective adsorption of Cr(VI). Experimental data showed adsorption process follows pseudo-second order kinetics. The TBA-SCC adsorbent has shown estimable adsorption capacity of 225.9 mg g^{-1} for hexavalent chromium. This can be attributed to the co-operation of electrostatic interaction and ion exchange phenomena at quaternary ammonium and sulphate ions sites of adsorbent,

Table 4 Comparison of adsorption capacity

Sl. no.	Adsorbents	Degree of deacetylation (%)	Adsorption capacity (mg g^{-1})	References
1.	Chitosan flakes	–	22.09	Aydin and Aksoy (2009)
2.	Aminated chitosan	90	28.7	Yan et al. (2007)
3.	Ethylene diamine modified chitosan	90	48.78	Hu et al. (2011)
4.	Sulphate-crosslinked chitosan	85	157	Kahu et al. (2014)
5.	Ionic liquid-impregnated chitosan	86.94	63.69	Kumar et al. (2012)
6.	TBA-SCC (present study)	85	225.9	(present study)

respectively. Adsorption process is spontaneous at room temperature for detoxifying hexavalent chromium. The reusability of TBA-SCC with high adsorption capacity makes it a greener material for Cr(VI) removal from industrial effluents.

Acknowledgments The authors are thankful to RTM Nagpur University for University Research Project No. Dev/1336 (2014–16).

References

Aydin YA, Aksoy ND (2009) Adsorption of chromium on chitosan: optimization, kinetics and thermodynamics. Chem Eng J 151:188–194

Bhatnagar A, Sillanpaa M (2009) Applications of chitin- and chitosan-derivatives for the detoxification of water and wastewater—a short review. Adv Colloid Interface Sci 152:26–38

Bulut E, Ozacar M, Sengil IA (2008) Adsorption of malachite green onto bentonite: equilibrium and kinetic studies and process design. Microporous Mesoporous Mater 115:234–246

Crini G, Peindy HN, Gimbert F, Robert C (2007) Removal of CI basic green 4 (Malachite Green) from aqueous solution by adsorption using cyclodextrin based adsorbent: kinetic and equilibrium studies. Sep Purif Technol 53:97–110

Debnath S, Maity A, Pillay K (2014) Magnetic chitosan-go nanocomposite: synthesis, characterization and batch adsorber design for Cr(VI) removal. J Environ Chem Eng 2:963–973

Devi MG, Al-Hashmi ZSS, Sekhar GC (2012) Treatment of vegetable oil mill effluent using crab shell chitosan as adsorbent. Int J Environ Sci Technol 9(4):713–718

Donia AM, Atia AA, El-Boraey HA, Mabrouk D (2006) Uptake studies of copper(II) on glycidyl methacrylate chelating resin containing Fe_2O_3 particles. Sep Purif Technol 49:64–70

Dubinin MM, Radushkevich LV (1947) The equation of the characteristic curve of the activated charcoal. Proc Acad Sci USSR Phys Chem Sect 55:331–337

Elwakeel KZ (2014) Removal of arsenate from aqueous media by magnetic chitosan resin immobilized with molybdate oxoanions. Int J Environ Sci Technol 11(4):1051–1062

Freundlich HMF (1906) Over the adsorption in solution. Z Phys Chem 57:385–470

Hayes BL (2004) Recent advances in microwave-assisted synthesis. Aldrichimica Acta 37(2):66–76

Ho YS (2006) Review of second-order models for adsorption systems. J Hazard Mater B 136:681–689

Houk KN, Leach AG, Kim SP, Zhang X (2003) Binding affinities of host–guest, protein–ligand, and protein-transition-state complexes. Angew Chem Int Ed 42:4872–4897

Hu XJ, Wang JS, Liu YG, Li X, Zeng GM, Bao ZL, Zeng XX, Chen AW, Long F (2011) Adsorption of chromium(VI) by ethylenediamine-modified cross-linked magnetic chitosan resin: isotherms, kinetics and thermodynamics. J Hazard Mater 185:306–314

Kahu S, Saravanan D, Jugade R (2014) Effective detoxification of hexavalent chromium using sulfate-crosslinked chitosan. Water Sci Technol 70:2047–2055

Kalidhasan S, Gupta PA, Cholleti VR, Kumar ASK, Rajesh V, Rajesh N (2012) Microwave assisted solvent free green preparation and physicochemical characterization of surfactant-anchored cellulose and its relevance toward the effective adsorption of chromium. J Colloid Interface Sci 372:88–98

Katz SA, Salem H (2006) The toxicology of chromium with respect to its chemical speciation: a review. J Appl Toxicol 13:217–224

Kumar ASK, Rajesh N (2013) Exploring the interesting interaction between grapheme oxide, Aliquat-336 (a room temperature ionic liquid) and chromium(VI) for wastewater treatment. RSC Adv 3:2697–2709

Kumar ASK, Gupta T, Kakan SS, Kalidhasan S, Manasi S, Rajesh V, Rajesh N (2012) Effective adsorption of hexavalent chromium through a three centre (3c) co-operative interaction with an ionic liquid and biopolymer. J Hazard Mater 239–240:213–224

Kumar ASK, Kumar CU, Rajesh V, Rajesh N (2014a) Microwave assisted preparation of *n*-butylacrylate grafted chitosan and its application for Cr(VI) adsorption. Int J Biol Macromol 66:135–143

Kumar ASK, Sharma S, Reddy RS, Barathi M, Rajesh N (2014b) Comprehending the interaction between chitosan and ionic liquid for the adsorption of palladium. Int J Biol Macromol 72:633–663

Kumar ASK, Jiang SJ, Tseng WL (2015) Effective adsorption of chromium(VI)/Cr(III) from aqueous solution using ionic liquid functionalized multiwalled carbon nanotubes as a super sorbent. J Mater Chem A. doi:10.1039/c4ta06948j

Kyzas GZ, Bikiaris DN (2015) Recent modifications of chitosan for adsorption applicatons: a critical and schematic review. Mar Drugs 13:312–337

Lagergren S (1898) Zur theorie der sogennanten adsorption geloster Stoffe. K. Sven. Vetenskapsakad. Handlingar 24:1–39

Langmuir I (1918) The adsorption of gases on plane surface of glass, mica and platinum. J Am Chem Soc 40:1361–1403

Lewinsky AA (2007) Hazardous materials and wastewater: treatment, removal and analysis. Nova Publishers, New York

Mayyas MA (2012) Properties of chitosan nanoparticles formed using sulphate anions as crosslinking bridges. Am J Appl Sci 9:1091–1100

Mendham VJ, Denny RC, Barnes JD, Thomas MJK (2002) Vogel's textbook of quantitative chemical analysis, 6th edn. Pearson Education, Singapore

Rajesh N, Krishna Kumar AS, Kalidhasan S, Rajesh V (2011) Trialkylamine impregnated macroporous polymeric sorbent for the effective removal of chromium from industrial wastewater. Chem Eng Data 56:2295–2304

Shekhawat A, Kahu S, Saravanan D, Jugade R (2015) Synergistic behavior of ionic liquid impregnated sulphate crosslinked chitosan towards adsorption of Cr(VI). Int J Biol Macromol 80:615–626

Shekhawat A, Kahu S, Saravanan D, Jugade R (2016) Assimilation of chitin with tin for defluoridation of water. RSC Adv. doi:10.1039/C6RA00014B

Tirgar A, Golbabaei F, Hamedi J, Nourijelyani K, Shahtaheri SJ, Moosavi SR (2006) Removal of airborne hexavalent chromium mist using chitosan gel beads as a new control approach. Int J Environ Sci Technol 3(3):305–313

Weber WJ, Morris JC (1963) Kinetics of adsorption on carbon from solution. J Sanit Eng Div Am Soc Civil Eng 89:3–60

Yan Z, Haijia S, Tianwei T (2007) Adsorption behaviors of the aminated chitosan adsorbent. Korean J Chem Eng 24:1047–1052

Zhu L, Liu Y, Chen J (2009) Synthesis of *N*-methylimidazolium functionalized strongly basic anion exchange resins for adsorption of Cr(VI). Ind Eng Chem Res 48:3261–3267